Received: 26 May 2019 | Revised: 30 July 2019 | Accepted: 17 August 2019

DOI: 10.1111/jace.16759

Journal of the American Ceramic Society

ORIGINAL ARTICLE

Microwave dielectric properties of temperature-stable zircon-type (Bi, Ce)VO_4 solid solution ceramics

Huan-Huan Guo[1,2] | **Di Zhou**[1,2] | **Wen-Feng Liu**[2] | **Li-Xia Pang**[3] | **Da-Wei Wang**[4] | **Jin-Zhan Su**[5] | **Ze-Ming Qi**[6]

[1]Electronic Materials Research Laboratory, Key Laboratory of the Ministry of Education & International Center for Dielectric Research, School of Electronic Science and Engineering, Xi'an Jiaotong University, Xi'an, China

[2]State Key Laboratory of Electrical Insulation and Power Equipment, Xi'an Jiaotong University, Xi'an, China

[3]Micro-optoelectronic Systems Laboratories, Xi'an Technological University, Xi'an, China

[4]Department of Materials Science and Engineering, University of Sheffield, Sheffield, UK

[5]International Research Centre for Renewable Energy, State Key Laboratory of Multiphase Flow in Power Engineering, Xi'an Jiaotong University, Xi'an, China

[6]National Synchrotron Radiation Laboratory, University of Science and Technology of China, Hefei, China

Correspondence
Di Zhou, Electronic Materials Research Laboratory, Key Laboratory of the Ministry of Education & International Center for Dielectric Research, School of Electronic and Information Engineering, Xi'an Jiaotong University, Xi'an 710049, China.
Email: zhoudi1220@gmail.com

Funding information
National Key Research and Development Program of China, Grant/Award Number: 2017YFB0406301; National Natural Science Foundation of China, Grant/Award Number: U1632146; Fundamental Research Funds for the Central University; State Key Laboratory of Electrical Insulation and Power Equipment, Grant/Award Number: EIPE19210; 111 Project of China, Grant/Award Number: B14040

Abstract

In the $(Bi_{1-x}Ce_x)VO_4$ $(0 \le x \le 1)$ system, we found that the $(Bi_{1-x}Ce_x)VO_4$ $(0 \le x \le 0.1)$ belongs to the monoclinic scheelite phase and the $(Bi_{1-x}Ce_x)VO_4$ $(0.7 \le x \le 1)$ belongs to the tetragonal zircon phase, while the $(Bi_{1-x}Ce_x)VO_4$ $(0.1 < x < 0.7)$ belongs to the mixed phases of both monoclinic scheelite and tetragonal zircon structure. Interestingly, two components with near-zero temperature coefficient of resonant frequency (TCF) appeared in this system. In our previous work, a near-zero TCF of ~+15 ppm/°C was obtained in a $(Bi_{0.75}Ce_{0.25})VO_4$ ceramic with a permittivity (ε_r) of ~47.9 and a Qf (Q = quality factor = 1/dielectric loss; f = resonant frequency) value of ~18 000 GHz (at 7.6 GHz). Furthermore, in the present work, another temperature-stable microwave dielectric ceramic was obtained in $(Bi_{0.05}Ce_{0.95})VO_4$ composition sintered at 950°C and exhibits good microwave dielectric properties with a ε_r of ~11.9, a Qf of ~22 360 GHz (at 10.6 GHz), and a near-zero TCF of ~+6.6 ppm/°C. The results indicate that this system might be an interesting candidate for microwave device applications.

KEYWORDS
dielectric properties, low temperature, solid solutions, X-ray methods

1 | INTRODUCTION

Microwave dielectric materials play a key role in global society, with a wide range of applications straddling terrestrial and satellite communications, including Internet of Things (IoT), software radio, GPS, DBS TV, environmental monitoring via satellite, etc. The temperature coefficient of resonance frequency (TCF) is one of the important parameters of microwave dielectric ceramics. The dielectric resonator generally uses the frequency of a certain vibration mode of dielectric ceramic as its center frequency. Therefore, in order to eliminate the temperature drift of the resonant frequency characteristic of the resonator, it is necessary to make the TCF close to zero.[1–7]

In 2000, Valant and Suvorov[8] first reported that $BiVO_4$ ceramic not only sinter at a low temperature (<900°C) but also exhibit excellent microwave dielectric properties, with a permittivity (ε_r) of ~68, a Qf (Q = quality factor = 1/dielectric loss; f = resonant frequency) value of ~6500 GHz, and a negative TCF of ~−260 ppm/°C. However, the large negative TCF will limit its application in microwave devices, thus, further studies to adjust the TCF of $BiVO_4$ ceramic to near zero are of great interest. In our previous work,[9] the $(Bi_{1-x}Ce_x)VO_4$ ($x \leq 0.6$) ceramics were prepared via a solid-state reaction method and a near-zero TCF (+15 ppm/°C) was obtained in a $(Bi_{0.75}Ce_{0.25})VO_4$ ceramic with a ε_r of ~47.9 and a Qf value of ~18 000 GHz. However, we have noticed that the $(Bi_{0.4}Ce_{0.6})VO_4$ has a TCF = +173 ppm/°C and the microwave dielectric properties of zircon-structured $CeVO_4$ were reported by Zuo et al[10] with a ε_r of ~12.3, a Qf value of ~41 460 GHz, and a negative TCF of ~−34.4 ppm/°C. Furthermore, from the pseudo phase diagram of the $(Bi_{1-x}Ce_x)VO_4$ system reported in the literature,[9,11] $(Bi_{1-x}Ce_x)VO_4$ should be a tetragonal zircon phase between $x = 0.6 \sim 1$. Therefore, there are possibilities to design a temperature-stable microwave dielectric ceramic in $(Bi_{1-x}Ce_x)VO_4$ ($0.6 < x < 1$) solid solutions.

In this investigation, the $(Bi_{1-x}Ce_x)VO_4$ ($0.7 \leq x \leq 0.95$) solid solution ceramics were synthesized by a conventional solid-phase reaction method to prepare a temperature-stable microwave dielectric ceramic with near-zero TCF. The structural evolution, sintering behaviors, microstructures, and microwave dielectric properties were investigated in detail.

2 | EXPERIMENTAL PROCEDURES

Proportionate amounts of reagent-grade starting materials of CeO_2 (99%), Bi_2O_3 (99%), and V_2O_5 (99%) were measured based on the stoichiometric formulation of $(Bi_{1-x}Ce_x)VO_4$ ($0.7 \leq x \leq 0.95$). Details of the processing can be found in our previous work.[9] Samples were sintered in the temperature range 870 ~ 970°C for 2 hours. The samples were investigated using room-temperature X-ray diffraction (XRD) with Cu*K*α radiation (Rigaku D/MAX-2400 X-ray diffractometry). The microstructure images of the $(Bi_{1-x}Ce_x)VO_4$ ($0.7 \leq x \leq 0.95$) ceramics were obtained by scanning electron microscopy (FEI Quanta F250). The selected area electron diffraction (SAED) and high-resolution transmission electron microscopy (HRTEM) images were measured using a transmission electron microscope (TEM) (JEM-2100 Electron Microscope) operated at 200 kV. The surface properties of the $(Bi_{0.05}Ce_{0.95})VO_4$ ceramic were characterized using X-ray photoelectron spectroscopy (XPS) on a Thermo Fisher ESCALAB Xi+. The infrared reflectivity spectra and Raman spectra were taken by a Bruker IFS 66v FTIR spectrometer (NSRL) and a LabRAM HR Evolution with laser excitation at 532 nm, respectively. The ε_r and Qf value of $(Bi_{1-x}Ce_x)VO_4$ ($0.7 \leq x \leq 0.95$) ceramics were obtained using a network analyzer (8720ES, Agilent). Since the TCF value was tested at the temperature ranging from 25°C to 85°C, the instruments used for the test were network analyzer and temperature chamber (Delta 9023, Delta Design). The formula for calculating TCF is as follows:

$$\mathrm{TCF}\left(\tau_f\right) = \frac{f_T - f_{T_0}}{f_{T_0} \times \left(T - T_0\right)} \times 10^6, \quad (1)$$

where f_{T_0} and f_T are the resonant frequencies at temperatures T_0 and T, respectively.

3 | RESULTS AND DISCUSSION

Figure 1A shows the XRD patterns of $(Bi_{1-x}Ce_x)VO_4$ ($0.7 \leq x \leq 0.95$) ceramics sintered at their optimum temperatures. It can be seen that the $(Bi_{1-x}Ce_x)VO_4$ ($0.7 \leq x \leq 0.95$) ceramics were crystallized in a zircon-type tetragonal structure and no second phase is found, which indicates that the zircon-type tetragonal structure (space group $I4_1/amd$) is stable in the $(Bi_{1-x}Ce_x)VO_4$ ($0.7 \leq x \leq 0.95$) ceramics. In order to study the crystal structure of $(Bi_{0.05}Ce_{0.95})VO_4$ ceramic in more detail, refinements were performed using GSAS software based on the XRD data recorded on $(Bi_{0.05}Ce_{0.95})VO_4$ ceramic powders. The refinement results indicate that the $(Bi_{0.05}Ce_{0.95})VO_4$ ceramic is a tetragonal zircon structure with a space group $I4_1/amd$ (No. 141) and the lattice parameters are $a = b = 7.3777(4)$ Å, $c = 6.4809(1)$ Å. Figure 1B shows the calculated and measured XRD patterns, and the illustration is schematic crystal structure of the $(Bi_{0.05}Ce_{0.95})VO_4$ ceramic. In addition, the refined atomic fractional coordinates are listed in Table 1. The goodness-of-fit of refinement (R_{wp}/R_{exp}) is 1.9. Furthermore, we also used TEM to further analyze the structure of $(Bi_{0.05}Ce_{0.95})VO_4$ ceramic. The SAED pattern and HRTEM images of $(Bi_{0.05}Ce_{0.95})VO_4$ ceramic recorded along the [010] zone axis are presented in Figure 1C,D. The HRTEM image demonstrates that the characteristic spacings of the (200) and (101) lattice planes of $(Bi_{0.05}Ce_{0.95})VO_4$ ceramic are 0.36 and 0.49 nm, respectively, which correspond well with the refined lattice parameters. The schematic diagram of crystal structure can be well matched with the HRTEM image, and the small dots shown in Figure 1D are oxygen atoms. All of these results are well matched, which confirm that $(Bi_{0.05}Ce_{0.95})VO_4$ ceramic belongs to the tetragonal zircon structure with a space group $I4_1/amd$ (No. 141).

The surface micromorphology of the $(Bi_{1-x}Ce_x)VO_4$ ($0.7 \leq x \leq 0.95$) ceramics was studied by scanning electron

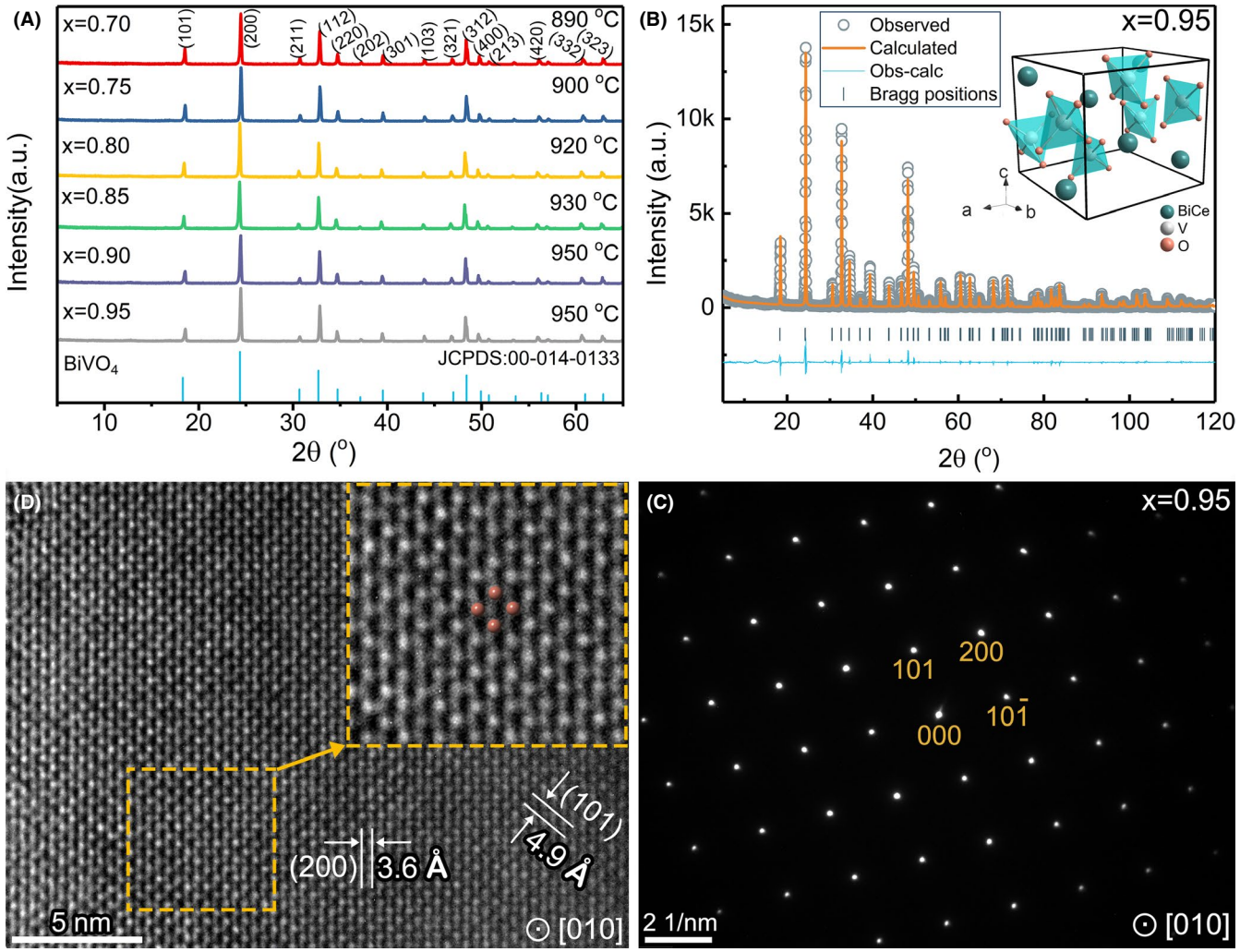

FIGURE 1 A, X-ray diffraction patterns of the $(Bi_{1-x}Ce_x)VO_4$ ($0.7 \le x \le 0.95$) ceramics sintered at optimal temperatures. B, The experimental (circle) and calculated (line) X-ray powder diffraction profiles for $(Bi_{0.05}Ce_{0.95})VO_4$ sample sintered at 950°C (the short vertical lines below the patterns mark the positions of Bragg reflections. The bottom continuous line is the difference between the observed and calculated intensity.). Insets is the schematic crystal structure of $(Bi_{0.05}Ce_{0.95})VO_4$. C and D, Selected area electron diffraction pattern and high-resolution transmission electron microscopy image of $(Bi_{0.05}Ce_{0.95})VO_4$ viewed along the [010] zone axis [Color figure can be viewed at wileyonlinelibrary.com]

TABLE 1 Refined atomic fractional coordinates from X-ray diffraction data of the $(Bi_{0.05}Ce_{0.95})VO_4$ ceramic and the cell parameters are $a = b = 7.3777(4)$ Å, $c = 6.4809(1)$ Å with a space group $I4_1/amd$ (No. 141)

Atom	Wyckoff position	Occ.	*x*	*y*	*z*	Biso
Bi	4a	0.05000	0.00000	0.75000	0.12500	0.00914
Ce	4a	0.95000	0.00000	0.75000	0.12500	0.00914
V	4b	1.00000	0.00000	0.25000	0.37500	0.00992
O	16 h	1.00000	0.00000	0.07309	0.20880	0.01314

microscopy (SEM). The SEM images of thermally etched surface of the $(Bi_{1-x}Ce_x)VO_4$ ($0.7 \le x \le 0.95$) ceramics sintered at optimal temperatures are shown in Figure 2A-F. Dense and homogeneous microstructures with almost no pores could be revealed in all compositions. Furthermore, the sintering temperatures of $BiVO_4$ and $CeVO_4$ ceramics are 820°C and 950°C, respectively.[8,10] So, the optimum sintering temperature of $(Bi_{1-x}Ce_x)VO_4$ ($0.7 \le x \le 0.95$) ceramics increased from 890°C to 950°C as x increased. This result indicates that the sintering temperatures of $CeVO_4$ ceramic can be lowered by the formation of solid solution and similar phenomena also exist in many other solid solution systems, such as $(1-x)BiVO_4$-$xLaNbO_4$, $(1-x)BiVO_4$-$xLa_{2/3}MoO_4$, $(Ca_{1-x}Bi_x)(Mo_{1-x}V_x)O_4$, and $(1-x)BiVO_4$-$x(Ag_{0.5}Bi_{0.5})MoO_4$ etc.[12–15]

A temperature-stable microwave dielectric ceramic with good microwave dielectric properties could be obtained at $x = 0.95$ (as discussed in Figure 5 below). Therefore, it is

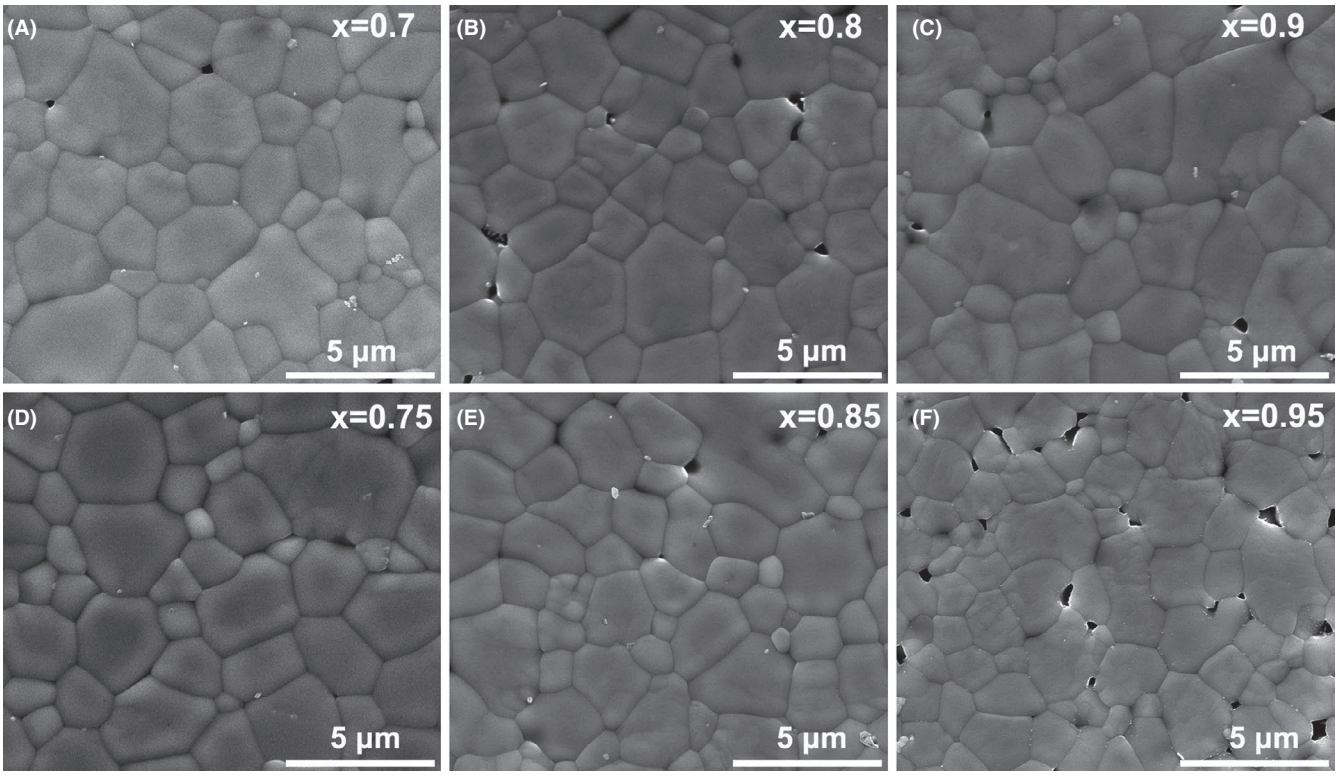

FIGURE 2 A-F, Scanning electron microscopy images of thermally etched surface of the $(Bi_{1-x}Ce_x)VO_4$ ($0.7 \le x \le 0.95$) ceramics sintered at optimal temperatures

necessary to study the $(Bi_{0.05}Ce_{0.95})VO_4$ ceramic in more detail. Raman spectroscopy is a good means to analyze the vibration modes of structural units such as [VO4]. Therefore, Raman spectroscopic investigation was also performed on $(Bi_{0.05}Ce_{0.95})VO_4$ ceramic. Pure $CeVO_4$ belongs to a tetragonal zircon structure with a space group $I4_1/amd$ and a point group D_{4h} (4/mmm). It is predicted by group theory that it has 12 distinct Raman active modes:

$$\Gamma = 2A_{1g} + 4B_{1g} + B_{2g} + 5E_g. \quad (2)$$

These vibration modes can be divided into two categories: internal models and external models. In $CeVO_4$, the vibration of the internal models is derived from the intermolecular vibration of the VO_4^{3-}. The vibration of each VO_4^{3-} anion is associated with other VO_4^{3-} ions in the same unit cell, resulting in abundant multi-vibration structure. One of the peaks shown in the spectrum may be due to the mixing of the vibrational compositions of different types of molecules. In order to observe the lattice vibration modes, the standard Gaussian-Lorentzian model was used to fit the Raman spectrum of $(Bi_{0.05}Ce_{0.95})VO_4$ ceramic to obtain the specific position information of all peaks. The fitted Raman spectra are presented in Figure 3A as red solid lines. As shown in Figure 3A, the strongest mode at 851 cm^{-1} is assigned as A_{1g} symmetric stretch (ν_1). The 777, 458, and 367 cm^{-1} Raman modes are assigned as E_g asymmetric stretch (ν_3), $E_g + B_{2g}$ deformation (ν_4), and $A_{1g} + B_{1g}$ deformation (ν_2), respectively. The B_{2g} mode at 254 cm^{-1} can be interpreted as symmetric bending of the $[VO_4]$ tetrahedron. Furthermore, the external modes appear at frequencies below 250 cm^{-1}. All vibration modes are consistent with the results reported in the previous literature.[9,16,17] The four normal vibration modes of tetrahedral $[VO_4]$ are shown in Figure 3B. In addition, Figure 3C shows the calculated and measured infrared reflectivity spectra of $(Bi_{0.05}Ce_{0.95})VO_4$ ceramic. The bands at 880, 788, and 259 cm^{-1} can be assigned as A_{2u} asymmetric stretch (ν_3), E_u asymmetric stretch (ν_3), and E_u deformation (ν_2), respectively. The weak band at 441 cm^{-1} is assigned as $E_u + A_{2u}$ deformation (ν_4). While the band at 176 cm^{-1} can be assigned to the Bi–O band (E_u). The infrared spectra of $(Bi_{0.05}Ce_{0.95})VO_4$ ceramic are similar to the reports in the literature.[9,17,18] In order to investigate the intrinsic microwave dielectric properties in detail, the infrared reflectivity spectra of $(Bi_{0.05}Ce_{0.95})VO_4$ ceramic were analyzed using a classical harmonic oscillator model:

$$\varepsilon^*(\omega) - \varepsilon(\infty) = \sum_{j=1}^{n} \frac{(z_j e)^2 \Big/ m_j V_j \varepsilon_0}{\omega_{Tj}^2 - \omega^2 - j\gamma_j \omega}, \quad (3)$$

where z_j is the equivalent price of the jth vibration mode, m_j is the equivalent mass of the jth vibrational mode, V_j is the equivalent unit volume of the jth vibrational mode, γ_j is the damping

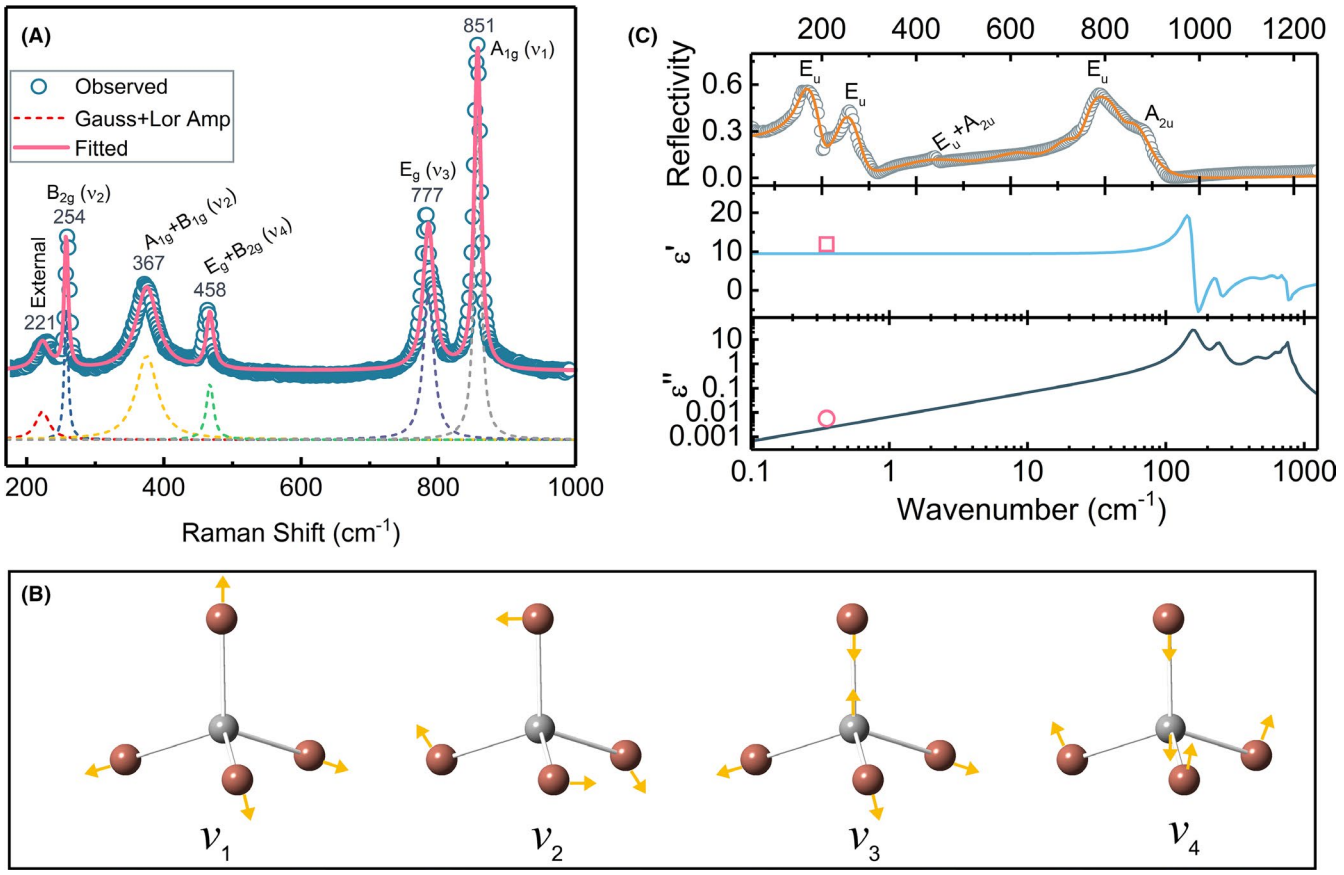

FIGURE 3 A, The experimental (circle) and calculated (black solid line) Raman spectra of $(Bi_{0.05}Ce_{0.95})VO_4$ ceramic sintered at 950°C (the short dot lines represent the Gaussian-Lorentzian fitting results). B, Four normal vibration modes of tetrahedral [VO_4]. C, Measured and calculated infrared reflectivity spectra (solid line for fitting values and circle for measured values) and fitted complex dielectric spectra of $(Bi_{0.05}Ce_{0.95})VO_4$ ceramic (square and circles are experimental in microwave region) [Color figure can be viewed at wileyonlinelibrary.com]

coefficient of the *j*th vibrational mode, ω_{Tj} is the angular frequency of the transverse optical modes of the *j*th mode of vibration, and n is the number of transverse phonon modes. The relation between complex reflectivity R(ω) and dielectric constant can be written as follows:

$$R(\omega) = \left| \frac{1 - \sqrt{\varepsilon^*(\omega)}}{1 + \sqrt{\varepsilon^*(\omega)}} \right|^2 . \quad (4)$$

Figure 3C shows the fitted infrared reflectivity values and the complex permittivities, and Table 2 lists the relevant parameters. It can be seen that the measured values (using the $TE_{01\delta}$ method) are very close to the calculated dielectric constant and dielectric loss values, indicating that in the microwave region, the dielectric polarization is mainly caused by phonon absorption in the infrared region.

X-ray photoelectron spectroscopy was used to characterize the chemical composition and oxidation state of each element in the $(Bi_{0.05}Ce_{0.95})VO_4$ ceramic. The XPS spectrum of $(Bi_{0.05}Ce_{0.95})VO_4$ sample with the survey and high-resolution spectrum of all elements are shown in Figure 4A-E. It is seen that the survey spectrum (Figure 4A) revealed the presence of Bi, Ce, V, and O in $(Bi_{0.05}Ce_{0.95})VO_4$. In the Ce 3d spectrum (Figure 4C), the peaks at 881.8 and 885.9 eV correspond to the Ce $3d_{5/2}$ transitions, while the peaks at 900.2 and 904.3 eV belong to the Ce $3d_{3/2}$ binding energy. The binding energies at 885.9 and 904.3 eV represent the $3d^{10}4f^1$ initial electronic state corresponding to Ce^{3+} and no peak associated with Ce^{4+} was found, which is consistent with the results of $CeVO_4$ reported in the literature.[19,20] The

TABLE 2 Phonon parameters obtained from the fitting of the infrared reflectivity spectra of $(Bi_{0.05}Ce_{0.95})VO_4$ ceramic

Mode	ω_{oj}	ω_{pj}	γ_j	$\Delta\varepsilon_j$
1	158.60	340.24	29.10	4.60
2	241.10	249.53	39.76	1.07
3	463.28	332.93	161.81	0.52
4	622.37	402.31	120.87	0.42
5	716.04	416.28	67.75	0.34
6	761.22	411.21	37.79	0.29
7	845.58	108.77	47.00	0.02
$(Bi_{0.05}Ce_{0.95})VO_4$	$\varepsilon_\infty = 2.23$		$\varepsilon_0 = 9.48$	

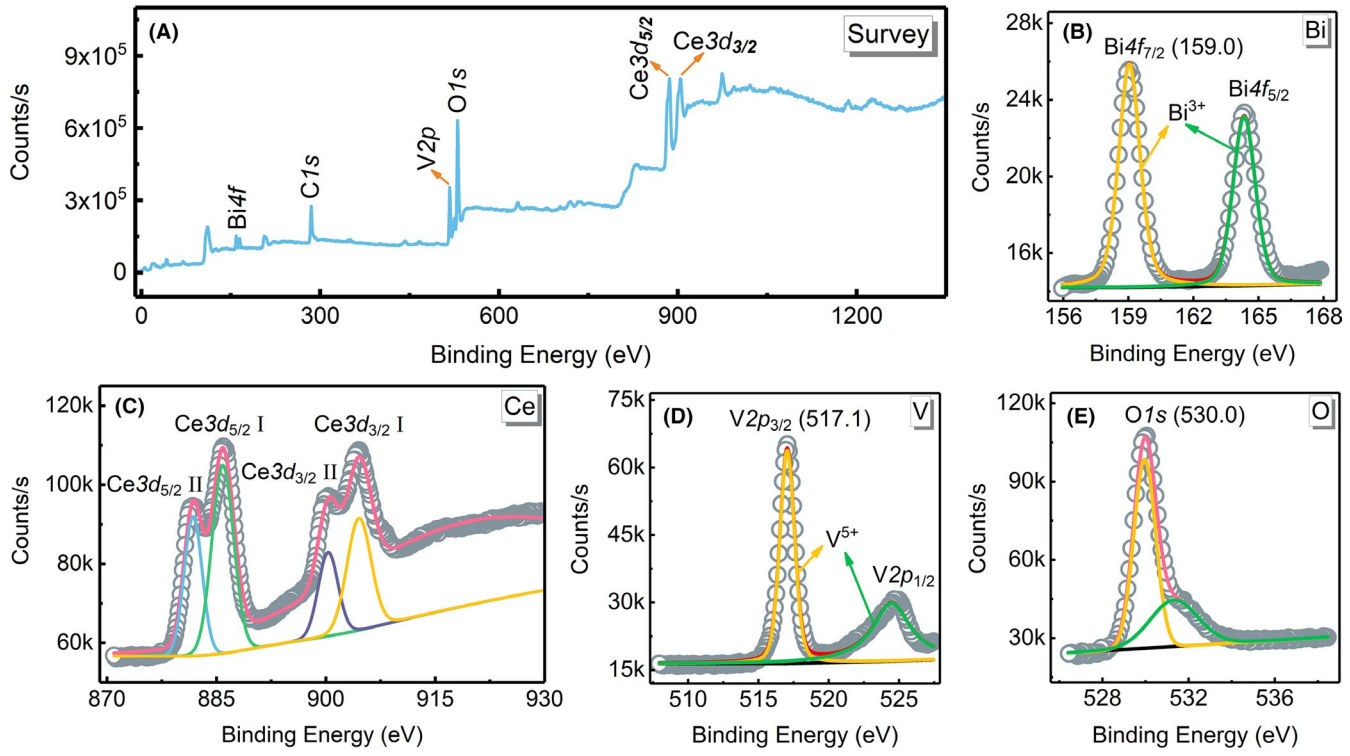

FIGURE 4 X-ray photoelectron spectroscopy spectra of $(Bi_{0.05}Ce_{0.95})VO_4$ ceramic with (A) the survey spectrum and high-resolution spectra of (B) Bi 4*f*, (C) Ce 3*d*, (D) V 2*p*, and (E) O 1*s* (all peaks have been calibrated with respect to the C 1*s* peak at 284.8 eV) [Color figure can be viewed at wileyonlinelibrary.com]

V 2*p* spectrum exhibits two contributions, $2p_{3/2}$ and $2p_{1/2}$ (resulting from the spin-orbit splitting), located at, respectively, 517.1 and 524.6 eV, which can be matched well with V_2O_5.[21] The Bi $4f_{7/2}$ peak at 159.0 eV agreed with the peak position of $BiVO_4$ in the literature,[22] and the peak located at 530.0 eV can be assigned to O 1*s* of O^{2-}.[23] These results indicated that the oxidation states of Bi, Ce, and V in the $(Bi_{0.05}Ce_{0.95})VO_4$ sample were +3, +3, and +5, respectively.

According to our previous work,[9] we found that the TCF of $BiVO_4$ can be adjusted from −260 ppm/°C to near zero (+15 ppm/°C) when the substitution amount of Ce is 0.25 in the $(Bi_{1-x}Ce_x)VO_4$ $(0 \le x \le 0.6)$ ceramics. However, we also noticed that the TCF of $(Bi_{0.4}Ce_{0.6})VO_4$ ceramic is +173 ppm/°C, while Zuo et al reported that the TCF of $CeVO_4$ ceramic is −34.4 ppm/°C.[10] Therefore, another component with a near-zero TCF will appear in $(Bi_{1-x}Ce_x)VO_4$ $(0.6 < x < 1)$ ceramics, which prompted us to find such a temperature-stable microwave dielectric ceramic. To better understand how microwave dielectric properties change with the substitution of Ce for Bi, the microwave dielectric properties, ε_r, Qf, and TCF, of the $(Bi_{1-x}Ce_x)VO_4$ $(0 \le x \le 1)$ ceramics sintered at their respective optimum temperatures as a function of *x* value are presented in Figure 5A-C. Among them, the data of $(Bi_{1-x}Ce_x)VO_4$ $(0 \le x \le 0.6)$ ceramics are taken from our previous work,[9] and the data of $(Bi_{1-x}Ce_x)VO_4$ $(0.7 \le x \le 0.95)$ ceramics come from this work. In addition, the data of $CeVO_4$ ceramic are taken from the literature reported by Zuo et al[10] In order to make clear the changes of ε_r and Qf with *x* value, we performed a linear fit on them separately. It can be seen that the ε_r of samples decreases linearly with the increase of *x*, mainly because the ε_r depends on the molecular polarizability. It has been reported in previous literature that the ionic polarizability of Ce^{3+} is smaller than that of Bi^{3+} in the structural environment of monoclinic scheelite and tetragonal zircon phase, thus resulting in the ε_r of $(Bi_{1-x}Ce_x)VO_4$ $(0 \le x \le 1)$ decreases with the cerium content.[9] As plotted in Figure 5B, the Qf values decrease roughly with the increase of *x*. In other words, the Qf values are inversely proportional to the permittivities. It is due to the intrinsic dielectric loss caused by absorptions of phonon oscillation in the lattice is proportional to the ε_r and the optimum Qf value depends on the intrinsic dielectric loss based on the classical harmonic oscillator model. Therefore, the Qf value of $(Bi_{1-x}Ce_x)VO_4$ $(0 \le x \le 1)$ ceramics shows an increasing trend. At microwave region, the Qf value has inverse relation to ε_r[24]

$$\left(Q \times f \approx \frac{(ze)^2/mV\varepsilon_0}{2\pi\gamma \times (\varepsilon'(\omega) - \varepsilon(\infty))}\right).$$

This relation has successfully explained the relationship between the Qf and the ε_r of many scheelite solid solutions such as $(Bi_{1-x}Y_x)VO_4$, $[(Li_{0.5}Bi_{0.5})_{1-x}Ca_x]MoO_4$ and

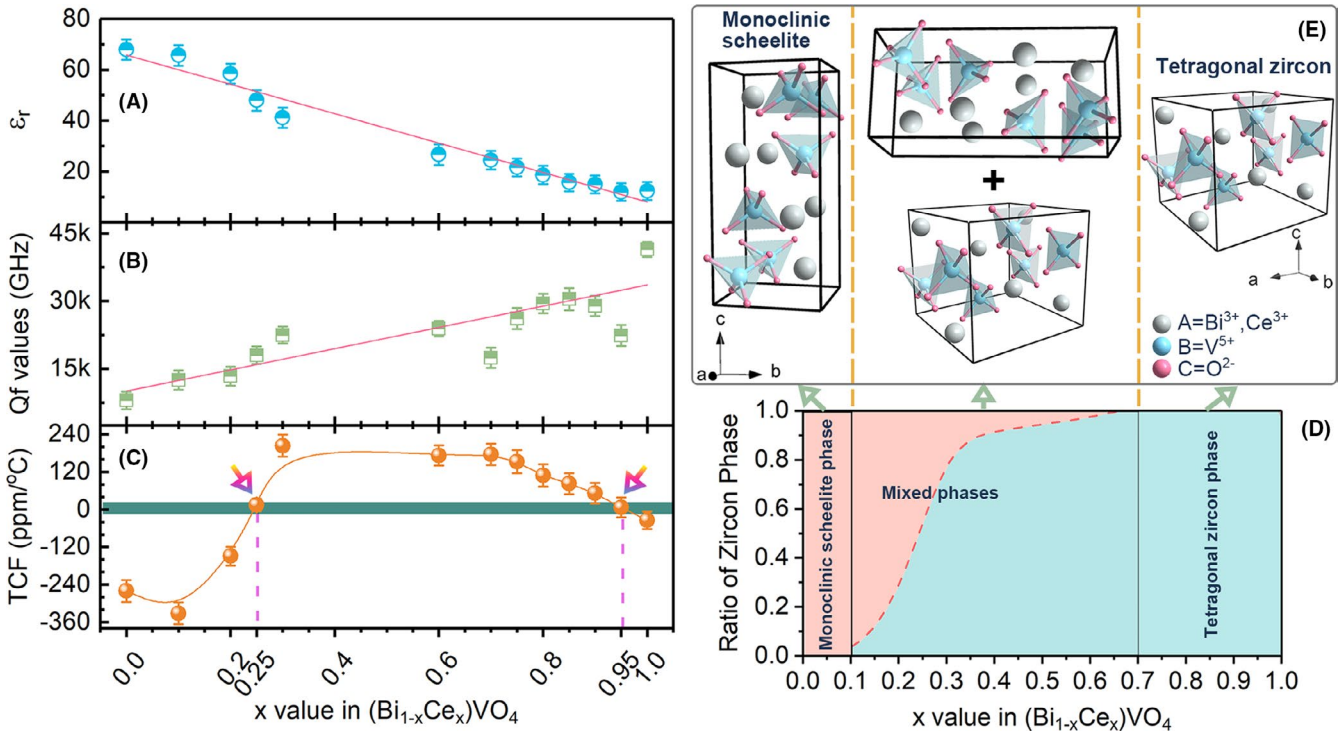

FIGURE 5 The microwave dielectric properties, ε_r (A), Qf (B) and resonant frequency (C), of $(Bi_{1-x}Ce_x)VO_4$ $(0 \le x \le 1)$ ceramics sintered at optimal temperatures as a function of x value. D, The pseudo phase diagram of the $(Bi_{1-x}Ce_x)VO_4$ system. The red dotted line represent the zircon phase contents in samples calculated by Fullprof software (detailed information on the calculation method is described in the literature[9]). E, The associated schematic crystal structures of each region in pseudo phase diagram [Color figure can be viewed at wileyonlinelibrary.com]

$(Ca_{1-x}Bi_x)(Mo_{1-x}V_x)O_4$.[15,18,24] Moreover, the facts show that the same qualitative relationship is also suitable for $(Bi_{1-x}Ce_x)VO_4$ $(0 \le x \le 1)$ ceramics. As presented in Figure 5C, the TCF first increases from a negative value to a positive value, and then decreases from a positive value to a negative value. Therefore, two component points with near-zero TCF appear in $(Bi_{1-x}Ce_x)VO_4$ $(0 \le x \le 1)$ ceramics, which are $x = 0.25$ and $x = 0.95$, respectively, indicating that the substitution of Ce for Bi in $BiVO_4$ is an effective method to adjust TCF to near zero. To understand the effect of sintering temperature on the TCF values of these two component points, the TCF of $(Bi_{0.75}Ce_{0.25})VO_4$ and $(Bi_{0.05}Ce_{0.95})VO_4$ ceramics as a function of sintering temperature is shown in Figure 6. It can be seen that the TCF of the $(Bi_{0.75}Ce_{0.25})VO_4$ and $(Bi_{0.05}Ce_{0.95})VO_4$ ceramics tends to decrease first and then remain stable as the sintering temperature increases. In order to better understand the crystal structure of the two components with near-zero TCF, the pseudo phase diagram of $(Bi_{1-x}Ce_x)VO_4$ $(0 \le x \le 1)$ ceramics and the associated schematic crystal structures of each region are shown in Figure 5D,E. It can be seen that the $(Bi_{1-x}Ce_x)VO_4$ $(0 \le x \le 0.1)$ belongs to the monoclinic scheelite phase and the $(Bi_{1-x}Ce_x)VO_4$ $(0.7 \le x \le 1)$ belongs to the tetragonal zircon phase, while the $(Bi_{1-x}Ce_x)VO_4$ $(0.1 < x < 0.7)$ belongs to the mixed phases of both monoclinic scheelite and tetragonal zircon structure. Thus, the two components with near-zero TCF belong to the mixed phases and the tetragonal zircon phase, respectively. It is important to note that the $(Bi_{0.05}Ce_{0.95})VO_4$ ceramic sintered at 950°C can exhibit good microwave dielectric properties, with a ε_r ~11.9, a Qf ~22 360 GHz (at 10.6 GHz), and a TCF ~+ 6.6 ppm/°C. In the microwave region, polarizability is the sum of both ionic and electronic

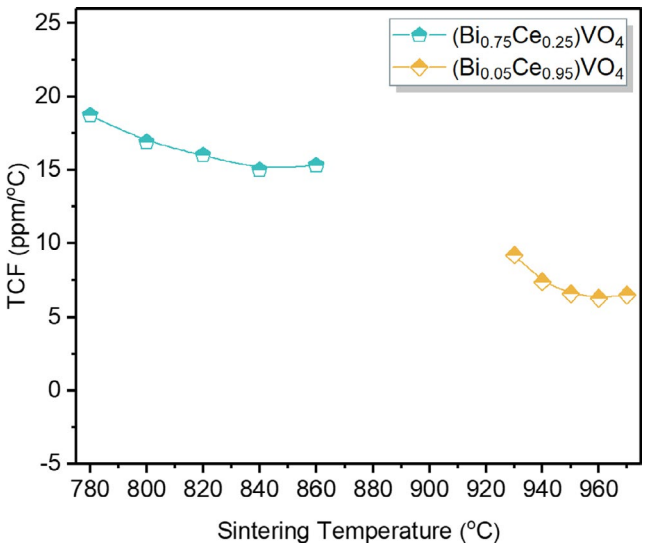

FIGURE 6 The resonant frequency of $(Bi_{0.75}Ce_{0.25})VO_4$ and $(Bi_{0.05}Ce_{0.95})VO_4$ ceramics as a function of sintering temperature [Color figure can be viewed at wileyonlinelibrary.com]

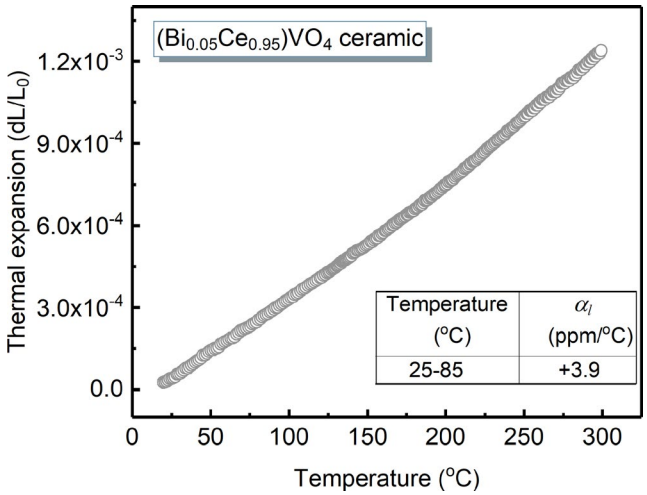

FIGURE 7 Thermal expansion data of the $(Bi_{0.05}Ce_{0.95})VO_4$ ceramic [Color figure can be viewed at wileyonlinelibrary.com]

components. Shannon[25] suggested that molecular polarizability (α) of complex substances maybe estimated by summing α of the constituent ions which for $(Bi_{0.05}Ce_{0.95})VO_4$ is:

$$\alpha_{Bi_{0.05}Ce_{0.95}VO_4} = 0.05\alpha_{Bi^{3+}} + 0.95\alpha_{Ce^{3+}} + \alpha_{V^{5+}} + 4\alpha_{O^{2-}} \approx 17.11\ \text{Å}, \quad (5)$$

where the ionic polarizabilities of Bi^{3+}, Ce^{3+}, V^{5+}, and O^{2-} are 6.12, 6.15, 2.92, and 2.01 $Å^3$, respectively.[25] Considering the Clausius-Mossotti relation,[26]

$$\varepsilon_{meas} = \frac{3V + 8\pi\alpha}{3V - 4\pi\alpha} \Rightarrow \alpha = \frac{3V\left(\varepsilon_{meas} - 1\right)}{4\pi\left(\varepsilon_{meas} + 2\right)} \approx 16.51\ \text{Å}^3, \quad (6)$$

where V is the cell volume (352.76/4 = 88.19 $Å^3$), the molecular polarizability may be obtained from ε_r to give ~16.51 $Å^3$ which is similar to the calculated value (17.11 $Å^3$) based on Shannon's additive rule. In addition, the TCF can be defined as follows:

$$\text{TCF} = -\left(\alpha_l + \frac{1}{2}\tau_\varepsilon\right), \quad (7)$$

where α_l is the thermal expansion coefficient and τ_ε is the temperature coefficient of the dielectric constant. According to the thermal expansion data (as shown in Figure 7), the α_l of $(Bi_{0.05}Ce_{0.95})VO_4$ ceramic is +3.9 ppm/°C between 25°C and 85°C. Hence, it can be calculated according to Equation 7 that τ_ε of the $(Bi_{0.05}Ce_{0.95})VO_4$ ceramic is −21.0 ppm/°C. In addition, using the Clausius-Mossotti relation, Bosman and Havinga[27] derived an expression for τ_ε at constant pressure as follows:

$$\begin{aligned}\tau_\varepsilon &= \frac{1}{\varepsilon}\left(\frac{\partial\varepsilon}{\partial T}\right)_p = \frac{(\varepsilon-1)(\varepsilon+2)}{\varepsilon}(\text{A}+\text{B}+\text{C}) \\ &= \left(\varepsilon - \frac{2}{\varepsilon} + 1\right)(\text{A}+\text{B}+\text{C}),\end{aligned} \quad (8)$$

$$\text{A} = -\frac{1}{3V}\left(\frac{\partial V}{\partial T}\right)_p, \quad \text{B} = \frac{V}{\alpha_m}\left(\frac{\partial \alpha_m}{\partial V}\right)_T \cdot \frac{1}{3V}\left(\frac{\partial V}{\partial T}\right)_p,$$
$$\text{C} = \frac{1}{3\alpha_m}\left(\frac{\partial \alpha_m}{\partial T}\right)_V.$$

The value of the A+B term is about 6 ppm/°C. Moreover, the term C generally lies between −1 and ~−10 ppm/°C and represents the direct dependence of the polarizability on temperature. According to Equation 8, the (A+B+C) value of the $(Bi_{0.05}Ce_{0.95})VO_4$ ceramic can be calculated to −1.6 ppm/°C, which is within an acceptable range.

4 | CONCLUSIONS

In the $(Bi_{1-x}Ce_x)VO_4$ ($0.7 \le x \le 0.95$) ceramics, tetragonal zircon-type structured solid solution was formed. As x increased from 0.7 to 0.95, the sintering temperature of $(Bi_{1-x}Ce_x)VO_4$ ($0.7 \le x \le 0.95$) ceramics increased from 890°C to 950°C, while the TCF decreased linearly from +176.3 to +6.6 ppm/°C. Importantly, the $(Bi_{0.05}Ce_{0.95})VO_4$ ceramic sintered at 950°C can exhibit good microwave dielectric properties, with a ε_r ~11.9, a Qf ~22 360 GHz (at 10.6 GHz), and a TCF ~+ 6.6 ppm/°C. It is proved that a temperature-stable microwave dielectric ceramic with zircon-type tetragonal phase can be obtained by the substitution of Ce for Bi in $BiVO_4$. This work presents a novel method to modify the TCF of $BiVO_4$-type materials. $(Bi_{0.05}Ce_{0.95})VO_4$ ceramic has a good potential for microwave equipment and devices with near-zero TCF.

ACKNOWLEDGMENTS

This work was supported by the National Key Research and Development Program of China (2017YFB0406301), the National Natural Science Foundation of China (U1632146), the Fundamental Research Funds for the Central University, the State Key Laboratory of Electrical Insulation and Power Equipment (EIPE19210), and the 111 Project of China (B14040). The authors thank the administrators in IR beamline workstation (BL01B) of National Synchrotron Radiation Laboratory (NSRL) for their help in the IR measurement and fitting. The SEM and TEM works were done at the International Center for Dielectric Research (ICDR), Xi'an Jiaotong University, Xi'an, China and the authors thank Ms Yan-Zhu Dai and Mr Chuan-Sheng Ma for their help in using SEM and TEM. We thank Ms Jiamei Liu at Instrument Analysis Center of Xi'an Jiaotong University for her assistance with XPS analysis.

ORCID

Di Zhou https://orcid.org/0000-0001-7411-4658

REFERENCES

1. Sebastian MT, Jantunen H. Microwave materials and applications. Chichester, UK: Wiley; 2017.
2. Eoh YJ, Hong JA, Kim ES. Effect of two-step sintering on the microwave dielectric properties of $Zn_{1.8}SiO_{3.8}$ ceramics. Ceram Int. 2015;41:S544–S550.
3. Li L, Chen XM, Fan XC. Microwave dielectric properties of $MgTiO_3$–$SrTiO_3$ layered ceramics. J Eur Ceram Soc. 2006;26(13):2817–21.
4. Jiang XW, Li CC, Su CX, Wei ZH, Fang L. Low temperature firing and microwave dielectric properties of $BaCaV_2O_7$ ceramics. Ceram Int. 2015;41(3):5172–6.
5. Shih YT, Jean JH. Low-fire processing of microwave BNBT-based high-k dielectric with Li_2O-ZnO-B_2O_3 glass. J Am Ceram Soc. 2013;96(12):3849–56.
6. Pang LX, Zhou D. Modification of $NdNbO_4$ microwave dielectric ceramic by Bi substitutions. J Am Ceram Soc. 2019;102(5):2278–82.
7. Lei W, Zou ZY, Chen ZH, Ullah B, Zeb A, Lan XK, et al. Controllable τ_f value of barium silicate microwave dielectric ceramics with different Ba/Si ratios. J Am Ceram Soc. 2018;101(1):25–30.
8. Valant M, Suvorov D. Chemical compatibility between silver electrodes and low-firing binary-oxide compounds: conceptual study. J Am Ceram Soc. 2000;83(11):2721–9.
9. Zhou D, Pang LX, Guo J, Qi ZM, Shao T, Wang QP, et al. Influence of Ce substitution for Bi in $BiVO_4$ and the impact on the phase evolution and microwave dielectric properties. Inorg Chem. 2014;53(2):1048–55.
10. Wang Y, Zuo R, Zhang C, Zhang J, Zhang T. Low-temperature-fired $ReVO_4$ (Re = La, Ce) microwave dielectric ceramics. J Am Ceram Soc. 2015;98(1):1–4.
11. Zhou D, Pang LX, Wang DW, Reaney IM. $BiVO_4$ based high k microwave dielectric materials: a review. J Mater Chem C. 2018;6(35):9290–313.
12. Pang LX, Zhou D, Qi ZM, Liu WG, Yue ZX, Reaney IM. Structure–property relationships of low sintering temperature scheelite-structured (1–x)$BiVO_4$-x$LaNbO_4$ microwave dielectric ceramics. J Mater Chem C. 2017;5(10):2695–701.
13. Pang LX, Zhou D, Liu WG, Qi ZM, Yue ZX. Crystal structure and microwave dielectric behaviors of scheelite structured $(1-x)BiVO_4$-$xLa_{2/3}MoO_4$ $(0.0 \le x \le 1.0)$ ceramics with ultra-low sintering temperature. J Eur Ceram Soc. 2017;38(4):1535–40.
14. Zhou D, Pang LX, Qi ZM. Crystal structure and microwave dielectric behaviors of ultra-low-temperature fired $x(Ag_{0.5}Bi_{0.5})MoO_4$–$(1-x)BiVO_4$ $(0.0 \le x \le 1.0)$ solid solution with scheelite structure. Inorg Chem. 2014;53(17):9222–7.
15. Guo HH, Zhou D, Pang LX, Qi ZM. Microwave dielectric properties of low firing temperature stable scheelite structured (Ca, Bi)(Mo, V)O_4 solid solution ceramics for LTCC applications. J Eur Ceram Soc. 2019;39(7):2365–73.
16. Hirata T, Watanabe A. A comparison between the Raman spectra of $Ce_{1-x}Ca_xVO_{4-0.5x}$ $(0 \le x \le 0.41)$ and $Ce_{1-x}Bi_xVO_4$ $(0 \le x \le 0.68)$. J Solid State Chem. 2001;158(2):264–7.
17. Krašovec UO, Orel B, Šurca A, Bukovec N, Reisfeld R. Structural and spectroelectrochemical investigations of tetragonal $CeVO_4$ and Ce/V-oxide sol-gel derived ion-storage films. Solid State Ionics. 1999;118(3–4):195–214.
18. Zhou D, Li J, Pang LX, Chen GH, Qi ZM, Wang DW, et al. Crystal structure, infrared spectra, and microwave dielectric properties of temperature-stable zircon-type (Y,Bi)VO_4 solid-solution ceramics. ACS Omega. 2016;1(5):963–70.
19. Costa-Coquelard C, Jegou P, Benattar JJ. Role of substrate wettability in the "bubble deposition method" applied to the $CeVO_4$ nanowire films. Langmuir. 2011;27(8):4397–402.
20. Shen Y, Huang Y, Zheng S, Guo X, Chen Z, Peng L, et al. Nanocrystals of $CeVO_4$ doped by metallic heteroions. Inorg Chem. 2011;50(13):6189–94.
21. Takagikawai M, Soma M, Onishi T, Tamaru K. The adsorption and the reaction of NH_3 and NO_x on supported V_2O_5 catal. Can J Chem. 2011;58(20):2132–7.
22. Schuhl Y, Baussart H, Delobel R, Le Bras M, Leroy J-M, Gengembre L, et al. Study of mixed-oxide catalysts containing bismuth, vanadium and antimony. Preparation, phase composition, spectroscopic characterization and catalytic oxidation of propene. J Chem Soc Faraday Trans 1. 1983;79(9):2055–69.
23. Barbaray B, Contour JP, Mouvier G. Effects of nitrogen dioxide and water vapor on oxidation of sulfur dioxide over vanadium pentoxide particles. Environ Sci Technol. 1978;12(12):1294–7.
24. Zhou D, Wang H, Wang QP, Wu XG, Guo J, Zhang GQ, et al. Microwave dielectric properties and Raman spectroscopy of scheelite solid solution $[(Li_{0.5}Bi_{0.5})_{1-x}Ca_x]MoO_4$ ceramics with ultra-low sintering temperatures. Funct Mater Lett. 2010;03(04):253–7.
25. Shannon RD. Dielectric polarizabilities of ions in oxides and fluorides. J Appl Phys. 1993;73(1):348–66.
26. Rysselberghe PV. Remarks concerning the Clausius-Mossotti Law. J Phys Chem. 1931;36(4):1152–5.
27. Bosman AJ, Havinga EE. Temperature dependence of dielectric constants of cubic ionic compounds. Phys Rev. 1963;129(4):1593–600.

How to cite this article: Guo H-H, Zhou D, Liu W-F, et al. Microwave dielectric properties of temperature-stable zircon-type (Bi, Ce)VO_4 solid solution ceramics. *J Am Ceram Soc*. 2020;103:423–431. https://doi.org/10.1111/jace.16759